Marek A. KSIĄŻEK*, Artur JANIK*

DYNAMICS OF ACTIVE BIOMECHANICAL MODELS OF SEATED HUMAN BODY AND THEIR VIBRATION ISOLATION SYSTEMS**

SUMMARY

In the paper the dynamic behaviour of the systems composed of active human body models (AHBM) and passive isolation systems (VIS) subjected to sinusoidal and random excitations was discussed. The two active human body biomechanical models ("back-off" and "back-on") obtained several years ago by the first author of the presented paper can be considered as active, linear, stable, lumped parameter and unidirectional dynamical systems. These models "seated" on passive vibration isolation systems (VIS) make new, coupled dynamical models (AHBM+VIS). In the first part of the presented paper the dynamical characteristics of the coupled, linear models (AHBM+VIS) were thoroughly analyzed. The new maps of poles distribution of characteristic equations of the systems composed of the coupled models show, that in some cases, these systems can be unstable. In the paper the stability areas were numerically estimated and graphically presented for the simplest, linear vibration isolation system. In the second part of the paper the influence of some chosen nonlinear elements injected into VIS on the amplitudes of chosen model mass accelerations and relative displacements between them was estimated, basing on the results obtained from the simulation approach. The simulation investigations were done for a sequence of time delay of the VIS reactions and sinusoidal excitations. The sinusoidal excitations had variable amplitudes and the frequencies corresponding to the first resonant frequency of the considered AHBM+VIS systems. The values of the corresponding amplitudes of output signals were compared. In chosen cases where the simulations were done for the random excitations the root mean square values of the output signals were compared. The obtained results were compared with the simplest linear VIS, graphically presented and discussed.

Keywords*: active biomechanical models, vibration isolation*

DYNAMIKA UKŁADU ZŁOŻONEGO Z AKTYWNEGO MODELU BIOMECHANICZNEGO CIAŁA SIEDZĄCEGO CZŁOWIEKA I PASYWNEGO UKŁADU WIBROIZOLACJI

W pracy przeprowadzono analizę numeryczną własności dynamicznych układu składającego się z aktywnego modelu biomechanicznego ciała siedzącego człowieka (AHBM) oraz pasywnego układu wibroizolacji (VIS) w wersji liniowej i nieliniowej, poddanego wymuszeniom harmonicznym i przypadkowym. Rozpatrzono dwie wersje modelu ciała siedzącego człowieka. Przeprowadzono numeryczną analizę stabilności układów AHBM – VIS w wersji liniowej. Na podstawie analizy symulacyjnej porównano wpływ wybranych nieliniowości wchodzących w skład pasywnego układu wibroizolacji (VIS) na wartości wybranych sił, przyspieszeń i przemieszczeń względnych układu całego układu AHBM – VIS.

1. INTRODUCTION

In most of scientific papers beginning from early sixties [2, 3, 4, 30], passing by seventies [7, 8, 11, 14, 21, 23, 24], eighties [1, 12, 26] up to the end of nineties [20, 27, 29, 30, 32], modeling of seated human operator's body subjected to vibration was concentrated on passive, lumped parameter mechanical structures developed on the basis of the results of experiments done with human beings in leading laboratories mainly in the USA, England, Japan, Germany and France. These models were built for the determined positions, functions and tasks of seated humans like heavy truck drivers, helicopter pilots, army and building vehicles operators.

It seems to be obvious that operator's position is constantly changed during his work. Due to the changes of work position, tension of muscles and other variable components the dynamic properties of the operator's body lead to varying in time and position different, constant parameters biomechanical models. Up to now there are no universal models of seated human body subjected to vibration excitations. All existing models are functional, built for a priori assumed target. In 1997 two theoretical, active biomechanical models of seated human body in "back-on" and "back--off" positions were developed by [15]. They were thoroughly described in [16, 17]. The other active model of seated human body was developed by Lewis and Griffin in [19]. In recent years some, physically realized dummies of seated human body were built [5]. The biomechanical models of seated human body are applied in estimations of operator's health, quality of chairs and assessment of properties of vibration isolation of different type of seats. They are considered as suitable approach for modeling and prototype design of complex systems composed of human body and seat. Such systems however have got new dynamic characteristics containing individual features of human body and coupled with it vibration isolation system. These characteristics become more interesting in case when the

* Institute of Applied Mechanics, Cracow University of Technology, Kraków, ksiazek@mech.pk.edu.pl; astronom@wp.pl
** This study was partially supported by Polish Scientific Research Committee, PB-1429/T07/2004/26

human body can be represented by active dynamic system. In general active systems are more complex than passive ones. They are in principle non-minimum phase structures with some zeros of their transmissibilities placed in the right-hand plane of the complex variable s. Vibration isolation of active and non-minimum phase biomechanical models becomes more difficult than vibration isolation of passive and minimum – phase models. The difficulties concern mainly stability and physical realizability of coupled active human body models (AHBM) seated on passive vibration isolation system (VIS). In the present paper the coupled dynamical system composed of the active "back-on" and "back-off" human body models seated on passive vibration isolation system was presented and numerically analyzed in Maple and simulation studies in MATLAB environments.

2. DYNAMICAL CHARACTERISTICS OF AHBM – VIS MODELS

2.1. General presentation and assumptions

The following two general assumptions have been made:

1) the human body can be represented by a multi-DOF, linear, time-invariant, lumped parameter and active biomechanical model;
2) input random excitations are considered as sinusoidal and random accelerations, supposed to be stationary, normal and ergodic, of the vibrating base described correspondingly by their amplitudes, r.m.s values and power spectral densities.

The general scheme of the AHBM with two versions of VIS system was shown in Figure 1, where $F(t)$ denotes the interaction force acting between the seat of mass m_0 and vibrating base considered as a source of sinusoidal or random excitations.

2.2. Presentation of AHBM

The two active biomechanical models of the seated human-body were synthesized in [15] for "back-off" and "back-on" positions on the basis of experimental data presented in [22]. The common structure of the "back-off" and "back-on" models, seat of mass m_0 and VIS were shown in Figure 1. The control forces for "back-off" and "back-on" models were expressed, after [16, 17] correspondingly by the formulae (1) and (2):

$$F_A = -k_{11}(x_1 - x) - k_{12}(\dot{x}_1 - \dot{x}) - \\ -k_{13}(x_2 + x) - k_{14}(\dot{x}_2 + \dot{x}) \tag{1}$$

$$F_A = -k_{11}(x_1 + x) - k_{12}(\dot{x}_1 - \dot{x}) - \\ -k_{13}(x_2 + x) - k_{14}(\dot{x}_2 - \dot{x}) \tag{2}$$

Table 1 lists the AHBM parameters for two versions of human body models.

2.3. Resonance frequencies the AHMB – VIS system

Poles distribution and corresponding resonance frequencies of "back-off" and "back-on" AHBM and coupled AHBM – passive VIS, are listed in Table 2. The VIS was considered as the Kelvin – Voigt model joined with seat mass m_0. The following values of the parameters of the VIS were assumed for further considerations: damping coefficient α_m = 260 [Ns/m], coefficient of spring stiffness c_m = 9950 [N/m] and seat mass m_0 = 35 [kg].

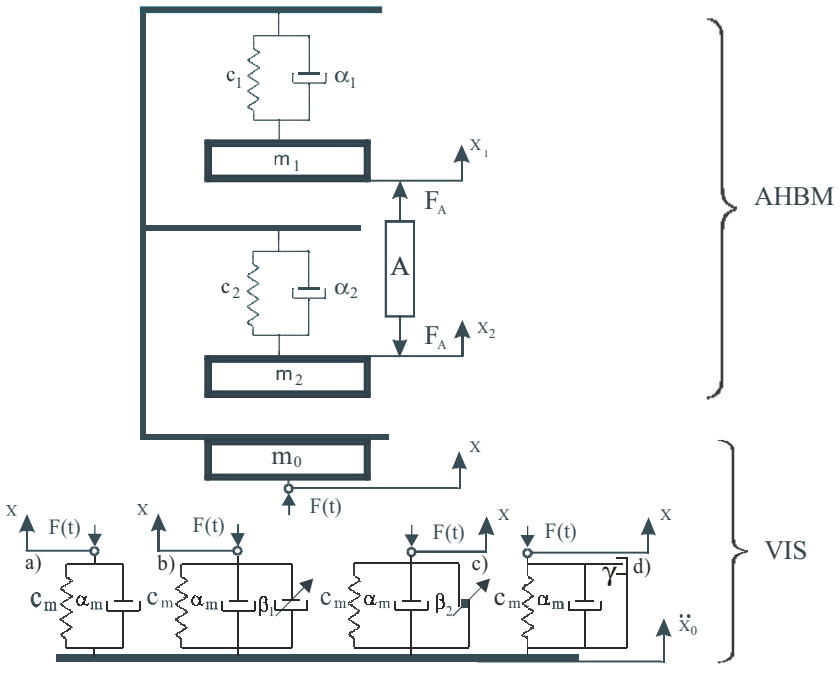

Fig. 1. Active Human Body Model (AHBM) and sequence of linear and non-linear Vibration Isolation System (VIS)

Table 1. AHBM parameters for two versions of human body models

Parameters of models	"Back-off" (z=3,p=4), m_1+m_2=70.8[kg]	Parameters of models	"Back-on" (z=3,p=4), m_1+m_2=70.8 [kg]
m_1 [kg]	9.1	m_1 [kg]	66
k_1 [N/m]	11972.5557	k_1 [N/m]	51189.32
α_1 [Ns/m]	3251.9783	α_1 [Ns/m]	1704.17
m_2 [kg]	61.7	m_2 [kg]	4.8
k_2 [N/m]	22456.7485	k_2 [N/m]	63335.50
α_2 [Ns/m]	519.0440	α_2 [Ns/m]	1262.59
k_{11} [N/m]	97323.2354	k_{11} [N/m]	123251.32
k_{12} [Ns/m]	-2226.0653	k_{12} [Ns/m]	-1781.04
k_{13} [N/m]	-1960.5176	k_{13} [N/m]	-104227.69
k_{14} [Ns/m]	1164.3525	k_{14} [Ns/m]	759.69

Table 2. Poles distribution and corresponding resonance frequencies of "back-off" and "back-on" AHBM and coupled AHBM – passive VIS

Model	r_1	ω_0 ω_d	r_2	ω_0 ω_d	r_3	ω_0 ω_d
Units		[Hz]		[Hz]		[Hz]
"Back-off" m_1=9.1 ,m_2=61.7 [kg]	-7,42+i8,25 -7,42-i8,25	11,1 8,25	-0,72+i4,74 -0,72-i4,74	4,80 4,74	– –	– –
"Back-off" +VIS m_0=35, m_1=9.1 ,m_2=61.7 [kg]	-15,8+i11.8 -15,8-i11.8	19,7 11,8	-1,33+i4,48 -1,33-i4,48	4,68 4,48	-0,173+i1,54 -0,173-i1,54	1,55 1,54
"Back-on" m_1=66, m_2=4.8 [kg]	-5,52+i26,5 -5,52-i26,5	27,1 26,5	-2,73+i6,14 -2,73-i6,14	6,72 6,14	– –	– –
"Back-on" + VIS m_0=35, m_1=66, m_2=4.8 [kg]	-0,84+i21,1 -0,84-i21,1	21,117 21,1	-14,5+i1,86 -14,5-i1,86	14,7 1,86	-0,201+i1,57 -0,201-i1,57	1,58 1,57

2.4. Numerical approach to problem of stability of coupled AHBM – VIS systems

One can show that each of the components of AHBM and VIS separately analysed, is stable. The coupled AHBM – VIS linear system has got different dynamic characteristics than their components AHBM and VIS and in some cases it becomes instable. In this paragraph the stability of coupled systems composed of "back-off" and "back-on" and passive VIS models were investigated. The stability area were numerically estimated on the basis of Hurwitz and poles distribution criteria, in terms of dimensionless damping coefficient $\alpha_m/260$ and mass m_0, for four values of the spring stiffness: $0.1c_m$, c_m, $2c_m$, $4c_m$. It was concluded, that the system composed of "back-on" AHBM and passive VIS becomes instable for some ranges of VIS parameters.

The stability and instability areas for such system were numerically estimated and presented in Figure 2 in terms of the VIS parameters m_0, α_m, c_m. Figure 2 shows big influence of parameters m_0 and α_m and small influence of the parameter c_m on the stability of the considered system.

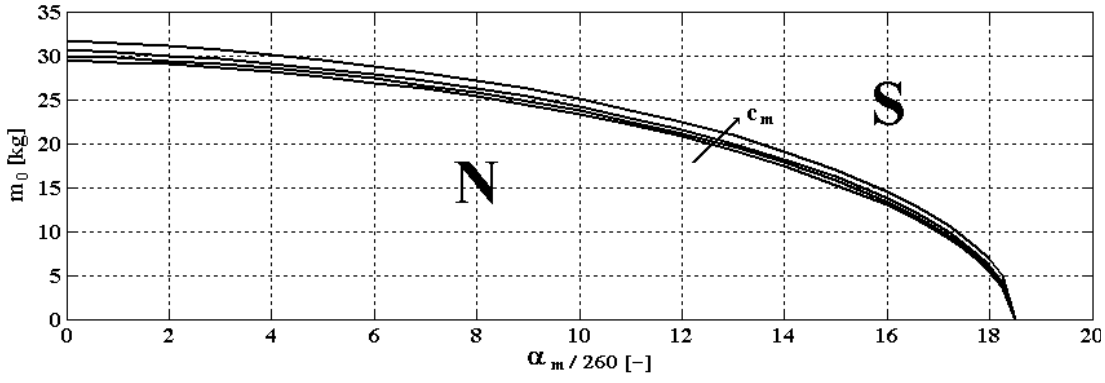

Fig. 2. Stability study of the coupled system: "back-on" AHBM-VIS, *N* – area of instability, *S* – area of stability

3. DYNAMICS OF AHBM – VIS NON-LINEAR MODELS SUBJECTED TO SINUSOIDAL EXCITATION

3.1. Nonlinearities introduced to VIS

The real VIS is a very complicated system. It is composed of seat and backrest cushions and a mechanical system composed of springs and dampers. There are many ideas of design of suspension seat models [6, 9, 25, 28]. In principle, such models consist of linear suspension spring, a non-linear asymmetrical damper force-velocity characteristic, a linear stiffness force simulating the damper gas preload, the effect of the damper geometry, a two state suspension friction force causing a constant force opposing the motion or a force just sufficient to hold the suspension mechanism stationary, non-linear stiffness elements for the end-stop buffers accounting for the geometrical arrangement of the buffers within the suspension and a rigid mass for the seat load. As one can conclude from the above the force coupling seated human body and suspension seat is a very complicated function of relative displacement $x - x_0$ and corresponding relative velocity $\dot{x} - \dot{x}_0$. For example in [10], this force is presented as the sum of two non-linear elastic and damping forces. The piecewise elastic force is described there by stiffness coefficient being composition of tan and fifth degree polynomial function of corresponding relative displacements. The damping force is described as a product of rela-tive velocity and a non-linear damping coefficient being fourth degree polynomial of relative displacement. Frequently, the dashpot resistance is more correctly expressed by a term proportional to the square of the relative velocity.

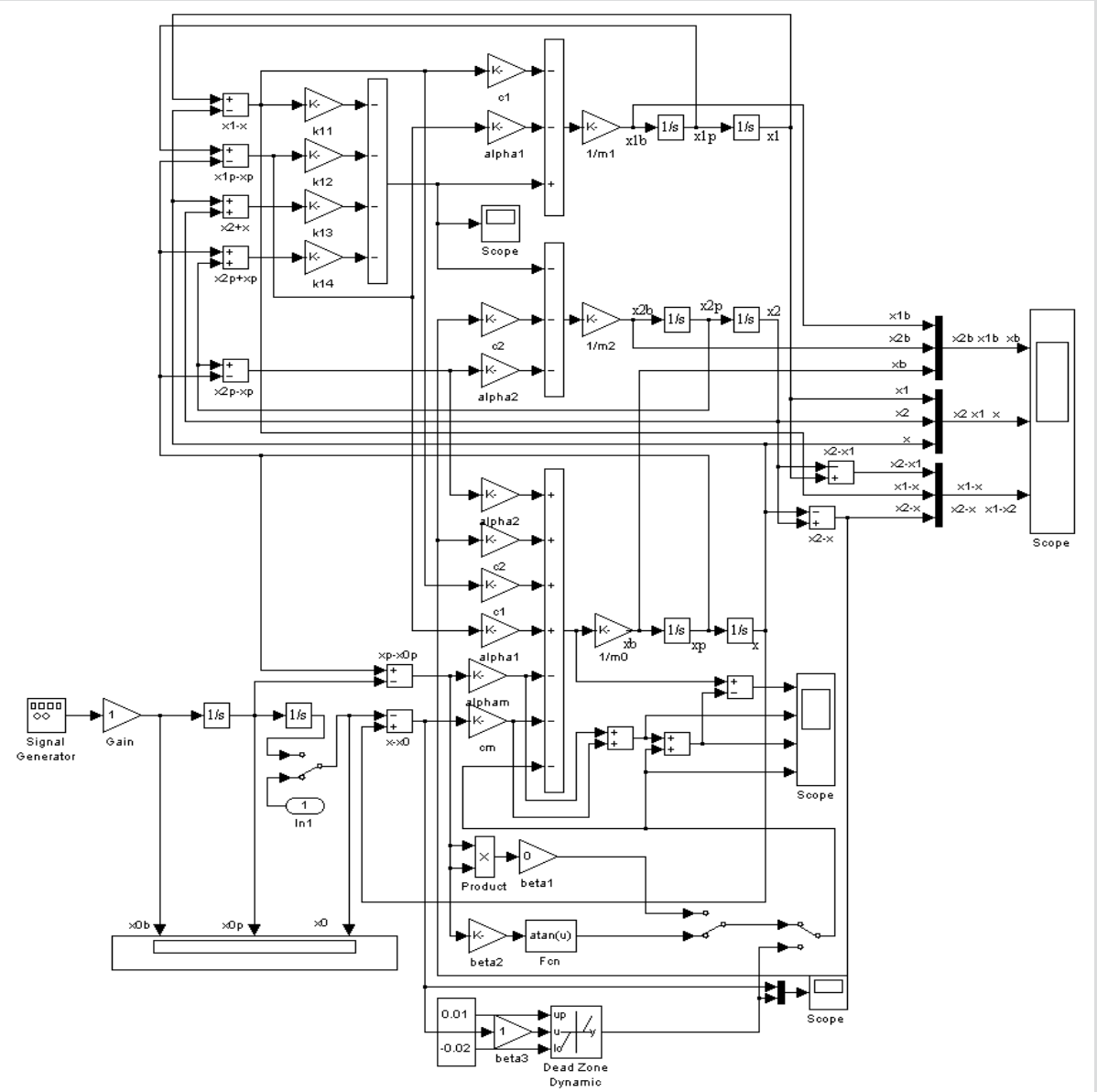

Fig. 3. Exemplary block diagram of simulation system composed of "back-on" model – linear VIS – and alternatively implemented non-linear elements presenting: quadratic damping (R) or Coulomb damping (T) or piecewise non-linear restoring force (F) expressed by formulae (3), (4) and (5)

In the present paper the following non-linearities shown in Figure 3, have been introduced into the VIS system:

– non-linear piece-wise restoring force:

$F = 0$ for $-b_1(x-x_0)b_2$

$F = \gamma(x-x_0)$ for $b_2(x-x_0)-b_1$ (3)

for b_1= 0.02 [m], b_2= 0.01 [m], γ = 0, 100, 200, 300, 400, 500, 600, 700, 800, 900, 1000 [N/m] taken as the mean values of asymmetric free travel zones and rigidities of the end-stop buffers of existing seats;

– non-linear damping force:

$$R = \beta_1 |\dot{x} - \dot{x}_0| (\dot{x} - \dot{x}_0) \quad (4)$$

with β_1 = 0, 50, 100, 200, 300, 400, 500, 600, 700, 800, 900, 1000 [Ns^2/m^2];

– non-linear Coulomb damping force:

$$T = \beta_2 \operatorname{sign}(\dot{x} - \dot{x}_0) \approx (2/\pi)\beta_2 \operatorname{atan}[1000(\dot{x} - \dot{x}_0)] \quad (5)$$

with β_2 = 0, 5, 10, 25, 50, 75, 100, 125, 150, 175, 200, 225, 250 [N].

3.2. Simulation studies

3.2.1. Block diagrams of the investigated systems

The simulation studies of the forced vibration of the AHBM+VIS system were done for some chosen non-linearities implemented in seat suspension. The system was subjected to sequence of sinusoidal and narrow band, random acceleration excitations, with equal r.m.s. values.

The simulation were done for both "back-off" and "back-on" seated human body models according to the exemplary block diagram presented in Figure 3. The final results were compared with the linear version of the system. In particular cases the influence of damping on the performance of suspension seating has been investigating using simulation studies and found to strongly influence predicted seat performance. Simulations of suspension seat dynamic performance therefore require the suspension damping to be known accurately. In the presented paper the simulation investigation were limited to some general models of restoring and damping forces and chosen sets of values of their parameters. Chosen numerical results of simulation were presented in graphical and numerical forms for: non-linear restoring force F (for "back-off" model in Figures 4–7 and Table 3, for "back-on" model in Figures 8–11 and Table 4), non-linear quadratic damping force R (for "back-off" model in Figures 12–15 and Table 5, for "back-on" model in Figures 16–19 and Table 6), non-linear coulomb force T (for "back-off" model in Figures 20–23 and Table 7, for "back-on" model in Figures 24 –27 and Table 8), correspondingly for the sinusoidal, acceleration excitation with amplitude equals to a_0 = 0.686 [m/s^2] r.m.s. and frequency equals to the first resonance frequency of the considered model.

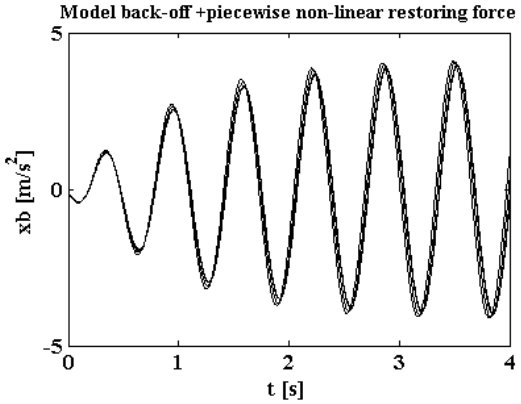

Fig. 4. Acceleration of mass $m_0 - \ddot{x}(t)$

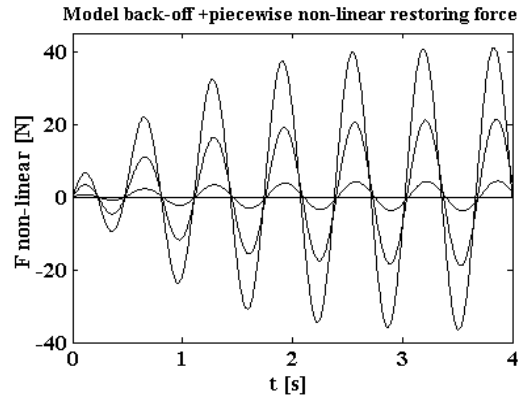

Fig. 5. Restoring force $F(t)$

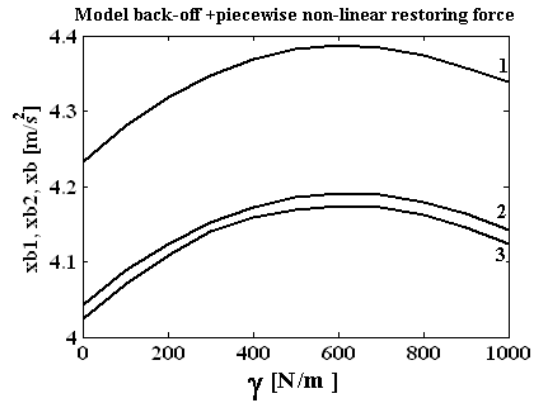

Fig. 6. Influence of parameter γ on accelerations:
$1-\ddot{x}_1; 2-\ddot{x}_2; 3-\ddot{x}$

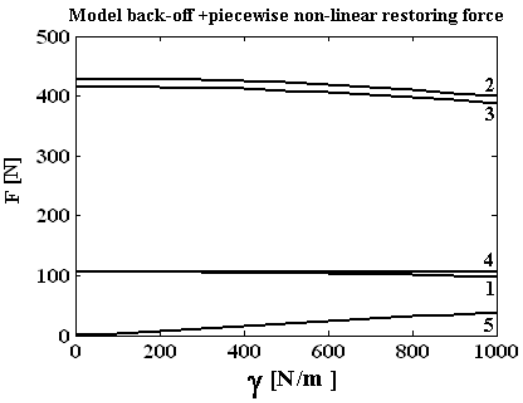

Fig. 7. Influence of parameter γ on forces:
$1-F_{\alpha_m}; 2-F_{c_m}; 3-F_{\alpha_m}+F_{c_m}; 4-F_{c_m}+F_{\gamma}; 5-F_{\gamma}$

Table 3. Numerical results of simulation for non-linear restoring force *F* ("back-off" model)

γ	xb_1	xb_2	xb	x_1	x_2	x	x_2-x_1	x_1-x	x_2-x	$F_{\alpha m}$	F_{cm}	$F_{\alpha m}$+ F_{cm}	F_{cm} +F_γ	F_γ
0	4,23	4,04	4,02	0,0446	0,0426	0,0423	0,01228	0,00904	0,00329	105,26	427,3	414,1	105,3	0,0
1	4,23	4,04	4,02	0,0446	0,0426	0,0424	0,01228	0,00904	0,00329	105,26	427,3	414,1	105,3	0,0
100	4,28	4,09	4,07	0,0451	0,0431	0,0428	0,01242	0,00914	0,00332	105,42	428,0	414,8	105,5	4,2
200	4,32	4,12	4,11	0,0455	0,0435	0,0432	0,01253	0,00922	0,00335	105,39	427,8	414,8	105,7	8,3
300	4,35	4,15	4,14	0,0459	0,0437	0,0435	0,01261	0,00929	0,00338	105,15	426,9	413,8	105,9	12,5
400	4,37	4,17	4,16	0,0461	0,0440	0,0437	0,01268	0,00933	0,00339	104,71	425,0	412,2	106,0	16,6
500	4,38	4,19	4,17	0,0462	0,0441	0,0438	0,01272	0,00936	0,00340	104,08	422,4	409,6	106,1	20,6
600	4,39	4,19	4,17	0,0463	0,0442	0,0439	0,01273	0,00937	0,00341	103,26	419,1	406,3	106,1	24,5
700	4,38	4,19	4,17	0,0462	0,0441	0,0439	0,01272	0,00937	0,00341	102,28	415,1	402,4	106,1	28,3
800	4,37	4,18	4,16	0,0461	0,0440	0,0438	0,01269	0,00934	0,00340	101,14	410,7	397,9	106,1	30,0
900	4,36	4,16	4,14	0,0459	0,0439	0,0436	0,01265	0,00931	0,00339	99,96	405,4	392,9	106,1	35,5
1000	4,34	4,14	4,12	0,0457	0,0437	0,0434	0,01259	0,00927	0,00337	98,71	399,9	387,6	106,1	38,9

3.2.2. Influence of piecewise non-linear restoring force (*F*)

Results of simulation of "back-off" model

In Figures 4 and 5 time histories of acceleration of mass m_0 and non-linear piecewise restoring force *F* depicted by the formula (3) are shown for four values of γ = 0, 100, 500, 1000 [N/m]. Figures 6 and 7 show correspondingly the influence of parameter γ on values of accelerations of all masses and forces developed by VIS for excitation acceleration amplitude equals to a_0.

Results of simulation of "back-on" model

In Figures 8 and 9 time histories of acceleration of mass m_0 and non-linear piecewise restoring force *F* are shown for four for four values of γ = 0, 100, 500, 1000 [N/m]. Figures 10 and 11 show correspondingly the influence of parameter γ on values of accelerations of all masses and forces developed by VIS for excitation acceleration amplitude equals to a_0.

3.2.3. Influence of quadratic damping force (*R*)

Results of simulation of "back-off" model

In Figures 12 and 13 time histories of acceleration of mass m_0 and non-linear quadratic damping force *R* depicted by the formula (4) are shown for four levels of acceleration excitation amplitudes a_0, $2a_0$, $4a_0$, $8a_0$. Figures 14 and 15 show correspondingly the influence of parameter β_1 on values of accelerations of all masses and forces developed by VIS.

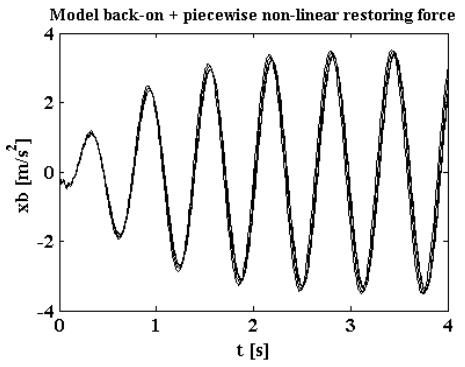

Fig. 8. Acceleration of mass $m_0 - \ddot{x}(t)$

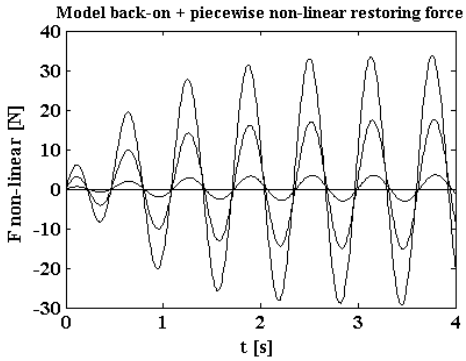

Fig. 9. Restoring force $F(t)$

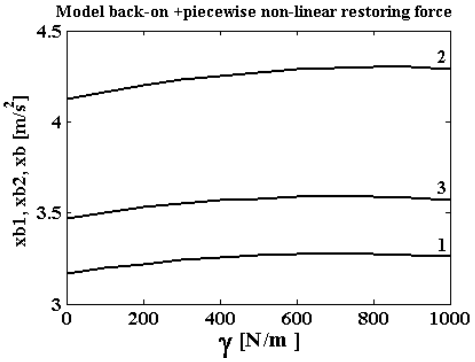

Fig. 10. Influence of parameter γ on accelerations:
$1-\ddot{x}_1; 2-\ddot{x}_2; 3-\ddot{x}$

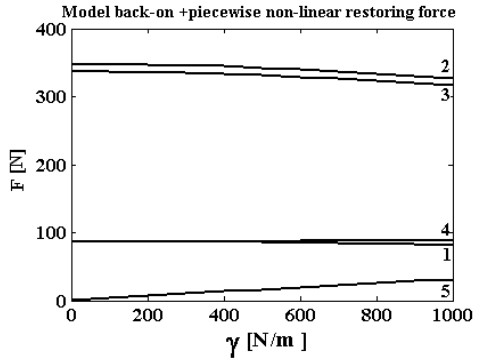

Fig. 11. Influence of parameter γ on forces:
$1-F_{\alpha_m}; 2-F_{c_m}; 3-F_{\alpha_m}+F_{c_m}; 4-F_{c_m}+F_\gamma; 5-F_\gamma$

Table 4. Numerical results of simulation for non-linear restoring force F ("back-on" model)

γ	xb_1	xb_2	xb	x_1	x_2	x	x_2-x_1	x_1-x	x_2-x	$F_{\alpha m}$	F_{cm}	$F_{\alpha m}$+ F_{cm}	F_{cm} +F_γ	F_γ
0	3,17	4,13	3,47	0,0320	0,0408	0,0349	0,00879	0,00296	0,00584	87,2	347,7	336,8	87,2	0
1	3,17	4,13	3,47	0,0320	0,0408	0,0349	0,00879	0,00296	0,00584	87,2	347,7	336,8	87,2	0,0
100	3,20	4,16	3,50	0,0323	0,0411	0,0352	0,00887	0,00299	0,00590	87,2	347,6	336,7	87,2	3,40
200	3,22	4,20	3,53	0,0325	0,0415	0,0355	0,00893	0,00301	0,00594	87,1	347,2	336,0	87,3	6,8
300	3,24	4,23	3,55	0,0327	0,0417	0,0357	0,00899	0,00303	0,00598	86,8	346,2	335,1	87,3	10,1
400	3,26	4,25	3,57	0,0329	0,0419	0,0359	0,00903	0,00305	0,00601	86,4	344,5	333,5	87,3	13,5
500	3,27	4,27	3,58	0,0330	0,0420	0,0360	0,00906	0,00306	0,00603	85,9	342,6	331,6	87,4	16,7
600	3,27	4,29	3,59	0,0331	0,0421	0,0361	0,00908	0,00306	0,00604	85,3	340,2	329,2	87,5	19,9
700	3,27	4,30	3,59	0,0331	0,0421	0,0361	0,00908	0,00306	0,00604	84,6	337,4	326,5	87,5	23,1
800	3,27	4,30	3,59	0,0330	0,0421	0,0361	0,00908	0,00306	0,00604	83,8	334,2	323,4	87,6	26,1
900	3,26	4,30	3,58	0,0330	0,0420	0,0360	0,00906	0,00306	0,00603	82,9	330,7	320,1	87,6	29,1
1000	3,26	4,29	3,57	0,0330	0,0419	0,0359	0,00904	0,00305	0,00601	82,0	326,9	316,5	87,7	31,9

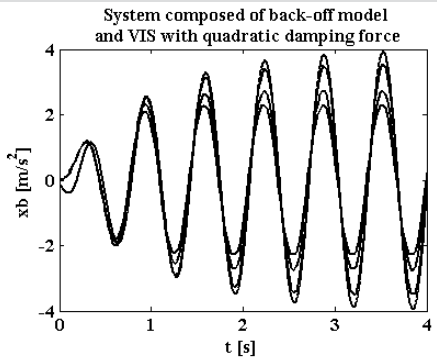

Fig. 12. Acceleration of mass $m_0 - \ddot{x}(t)$

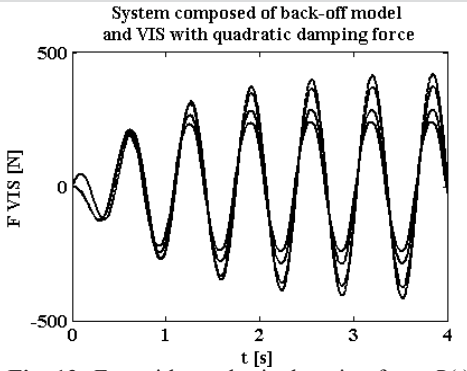

Fig. 13. F_{VIS} with quadratic damping force $R(t)$

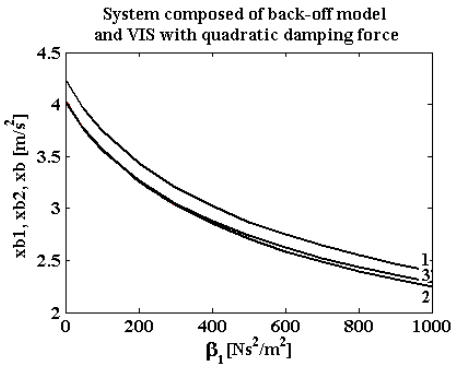

Fig. 14. Influence of parameter β_1 on accelerations: $1-\ddot{x}_1; 2-\ddot{x}_2; 3-\ddot{x}$

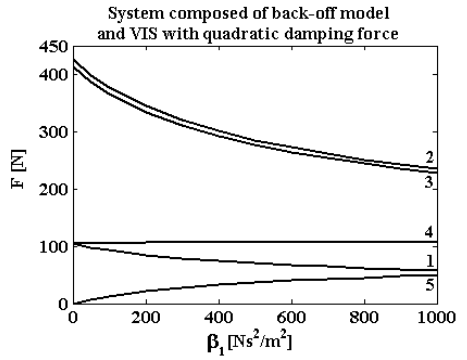

Fig. 15. Influence of parameter β_1 on forces: $1-F_{\alpha_m}; 2-F_{c_m}; 3-F_{\alpha_m}+F_{c_m}; 4-F_{\alpha_m}+F_{\beta_1}; 5-F_{\beta_1}$

Table 5. Numerical results of simulation for non-linear quadratic damping force R ("back-off" model)

β_1	xb_1	xb_2	xb	x_1	x_2	x	x_2-x_1	x_1-x	x_2-x	$F_{\alpha m}$	F_{cm}	$F_{\alpha m}$+ F_{cm}	$F_{\alpha m}$+$F_{\beta 1}$	$F_{\beta 1}$
0	4,23	4,04	4,01	0,0473	0,0452	0,0448	0,01325	0,00974	0,00356	105,2	426,6	413,6	105,2	0
50	3,96	3,78	3,76	0,0454	0,0433	0,0430	0,01273	0,00936	0,00343	98,1	398,9	386,9	105,2	7,1
100	3,75	3,57	3,56	0,0438	0,0418	0,0415	0,01229	0,0090	0,00332	92,8	376,9	365,8	105,5	12,7
200	3,44	3,26	3,27	0,0411	0.0393	0,0390	0,01157	0,00849	0,00313	84,7	344,6	334,0	106,0	21,3
300	3,20	3,03	3,05	0,0390	0,0373	0,0370	0,01099	0,00806	0,00298	79,0	320,3	310,5	106,6	27,7
400	3,02	2,86	2,87	0,0373	0,0356	0,0354	0,01052	0,00771	0,00286	74,1	301,2	292,0	106,6	32,5
500	2,87	2,71	2,74	0,0358	0,0342	0,0340	0,01011	0,00741	0,00275	70,4	285,4	276,9	107,1	36,7
600	2,75	2,59	2,62	0,0345	0,0330	0,0327	0,00977	0,00715	0,0026	67,2	272,6	264,3	107,3	40,1
700	2,64	2,48	2,52	0,0334	0.0319	0,0317	0,00947	0,0069	0,00259	64,4	261,4	253,4	107,3	42,9
800	2,55	2,40	2,43	0.0324	0,0310	0,0307	0,00920	0,00673	0,00252	61,9	251,4	244,0	107,3	45,4
900	2,47	2,32	2,36	0,0315	0,0301	0,0299	0,00896	0,00655	0,00246	59,8	243,0	235,6	107,4	47,6
1000	2,40	2,25	2,29	0,0307	0,0293	0,0291	0,00874	0,00639	0,00239	57,9	235,4	228,2	107,6	49,7

Results of simulation of "back-on" model

In Figures 16 and 17 time histories of acceleration of mass m_0 and non-linear piecewise restoring force F are shown for four levels of acceleration excitation amplitudes a_0, $2a_0$, $4a_0$, $8a_0$. Figures 18 and 19 show correspondingly the influence of the parameter β on values of accelerations of all masses of the AHBM – VIS model and forces developed by VIS.

3.2.4. Influence of Coulomb damping (*T*)

Results of simulation of "back-off" model

In Figures 20 and 21 time histories of acceleration of mass m_0 and non-linear coulomb force T depicted by the formula (5) are shown for four levels of acceleration excitation amplitudes a_0, $2a_0$, $4a_0$, $8a_0$. Figures 22 and 23 show correspondingly the influence of the parameter β_2 on values of accelerations of all masses of the AHBM – VIS model and forces developed by VIS.

Results of simulation of "back-on" model

In Figures 24 and 25 time histories of acceleration of mass m_0 and non-linear coulomb force T depicted by the formula (5) are shown for four levels of acceleration excitation amplitudes a_0, $2a_0$, $4a_0$, $8a_0$. Figures 26 and 27 show correspondingly the influence of the parameter β_2 on values of accelerations of masses of the AHBM – VIS model and forces developed by VIS.

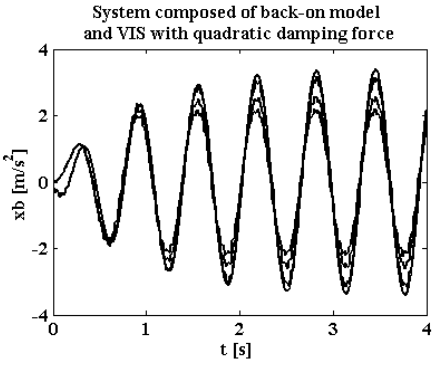

Fig. 16. Acceleration of mass $m_0 - \ddot{x}(t)$

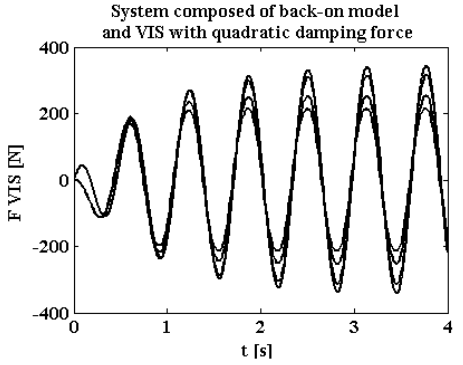

Fig. 17. F_{VIS} with quadratic damping force $R(t)$

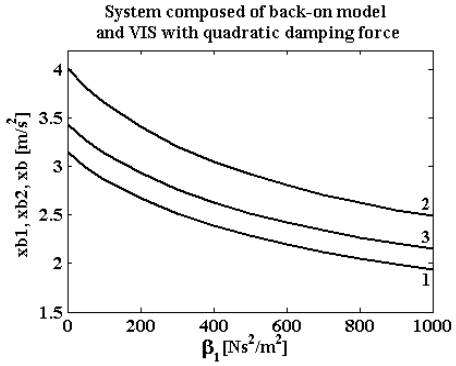

Fig. 18. Influence of parameter β_1 on accelerations: $1-\ddot{x}_1; 2-\ddot{x}_2; 3-\ddot{x}$

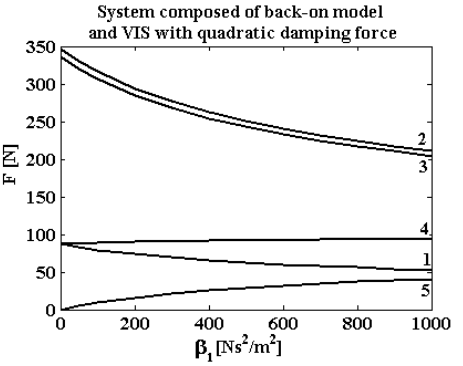

Fig. 19. Influence of parameter β_1 on forces: $1-F_{\alpha_m}; 2-F_{c_m}; 3-F_{\alpha_m}+F_{c_m}; 4-F_{\alpha_m}+F_{\beta_1}; 5-F_{\beta_1}$

Table 6. Numerical results of simulation for non-linear quadratic damping force R ("back-on" model)

β_1	xb_1	xb_2	xb	x_1	x_2	x	x_2-x_1	x_1-x	x_2-x	$F_{\alpha m}$	F_{cm}	$F_{\alpha m}$+ F_{cm}	$F_{\alpha m}$+$F_{\beta 1}$	$F_{\beta 1}$
0	3,15	4,01	3,43	0,0320	0,0408	0,0349	0,00879	0,00296	0,00584	87,1	347,1	336,0	87,1	0
50	2,99	3,8	3,27	0,0304	0,039	0,0332	0,00835	0,00282	0,00554	82,7	330,2	319,8	87,8	5,1
100	2,87	3,66	3,14	0,0291	0,0370	0,0317	0,00799	0,00270	0,00530	79,3	316,2	306,3	88,6	9,3
200	2,67	3,41	2,93	0,0269	0,0343	0,0294	0,00741	0,00251	0,00493	73,7	293,8	284,7	89,8	16,1
300	2,52	3,21	2,77	0,0252	0,0322	0,0276	0,00696	0,00236	0,00461	69,4	276,6	267,9	90,7	21,4
400	2,39	3,05	2,63	0,0240	0,0305	0,0262	0,00659	0,00224	0,00437	65,8	262,5	254,2	91,4	25,6
500	2,29	2,92	2,52	0,0228	0,0291	0,0249	0,00628	0,00214	0,00416	62,8	250,8	242,8	92,0	29,2
600	2,20	2,81	2,43	0,0219	0,0279	0,0239	0,00602	0,00205	0,00398	60,2	240,7	233,1	92,4	32,2
700	2,12	2,71	2,34	0,0210	0,0268	0,0230	0,00579	0,00197	0,00383	58,1	232,0	224,6	93,0	34,9
800	2,05	2,63	2,27	0,0203	0,0259	0,0222	0,00559	0,00190	0,00370	56,1	224,2	217,1	93,3	37,2
900	1,99	2,55	2,21	0,0196	0,0250	0,0215	0,00541	0,00184	0,00358	54,3	217,2	210,4	93,6	39,3
1000	1,94	2,49	2,15	0,0190	0,0243	0,0208	0,00524	0,00179	0,00347	52,7	211,0	204,4	93,8	41,1

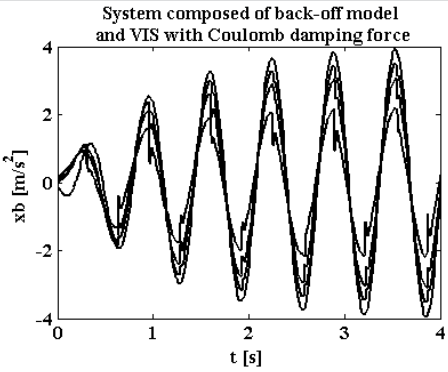

Fig. 20. Acceleration of mass $m_0 - \ddot{x}(t)$

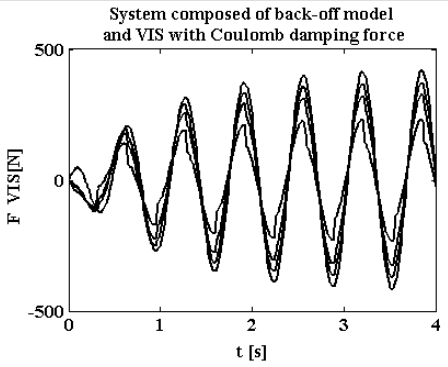

Fig. 21. F_{VIS} with Coulomb force $T(t)$

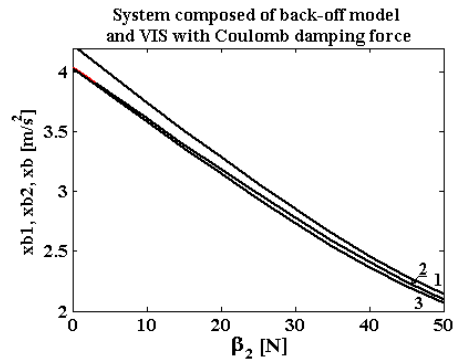

Fig. 22. Influence of parameter β_2 on accelerations: $1 - \ddot{x}_1; 2 - \ddot{x}_2; 3 - \ddot{x}$

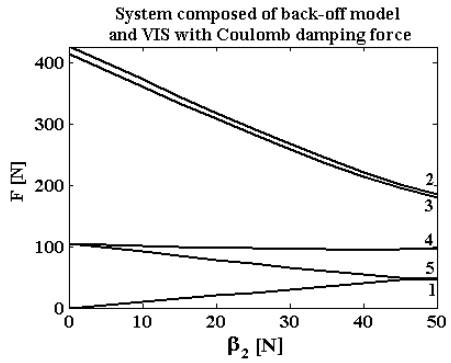

Fig. 23. Influence of parameter β_2 on forces: $1 - F_{\alpha_m}; 2 - F_{c_m}; 3 - F_{\alpha_m} + F_{c_m}; 4 - F_{\alpha_m} + F_{\beta_2}; 5 - F_{\beta_2}$

Table 7. Numerical results of simulation for non-linear Coulomb force T ("back-off" model)

β_2	xb_1	xb_2	xb	x_1	x_2	x	x_2-x_1	x_1-x	x_2-x	$F_{\alpha m}$	F_{cm}	$F_{\alpha m}$+ F_{cm}	$F_{\alpha m}$ +$F_{\beta 2}$	$F_{\beta 2}$
0	4,23	4,04	4,03	0,04464	0,04261	0,04235	0,01228	0,00904	0,003287	105,3	427,2	414,1	105,3	0
10	3,74	3,61	3,58	0,03918	0,03742	0,03715	0,01074	0,00791	0,002859	91,5	371,6	360,2	101,5	10,0
15	3,51	3,40	3,36	0,03650	0,03487	0,03461	0,00998	0,007360	0,002654	84,8	344,2	333,7	99,8	15,0
20	3,29	3,19	3,15	0,03387	0,03238	0,03211	0,00925	0,006820	0,002458	78,2	317,7	307,8	98,2	20,0
25	3,07	2,98	2,94	0,03131	0,02994	0,02968	0,00854	0,006295	0,002273	71,9	291,6	282,6	96,8	24,9
30	2,85	2,78	2,73	0,02885	0,02759	0,02734	0,00787	0,005793	0,002101	65,7	266,6	258,3	95,6	29,9
35	2,65	2,59	2,54	0,02651	0,02535	0,02511	0,00724	0,005321	0,001947	59,9	242,9	235,3	94,8	34,8
40	2,46	2,41	2,36	0,02432	0,02327	0,02304	0,00667	0,004888	0,001812	54,7	221,0	214,1	94,5	39,8
45	2,29	2,24	2,21	0,02233	0,02136	0,02117	0,00617	0,004508	0,001698	50,0	201,5	195,2	94,8	44,8
50	2,15	2,09	2,07	0,02058	0,01967	0,01951	0,00574	0,004188	0,001607	46,0	184,8	178,9	95,7	49,7

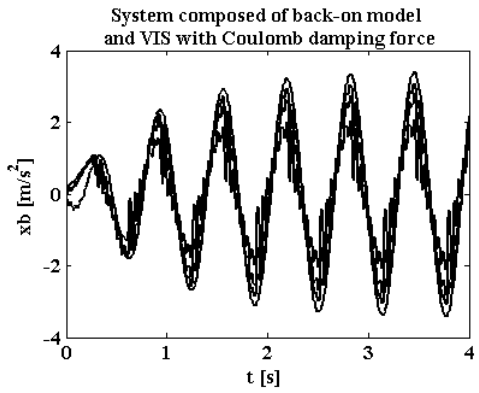

Fig. 24. Acceleration of mass $m_0 - \ddot{x}(t)$

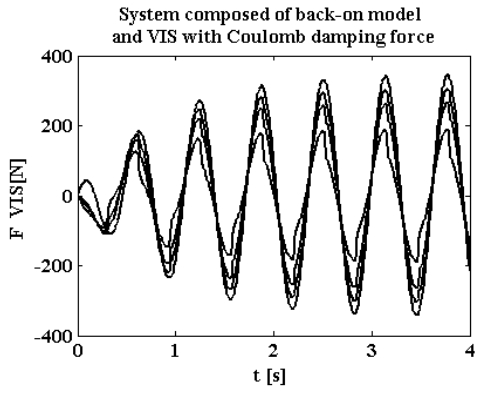

Fig. 25. F_{VIS} with Coulomb force $T(t)$

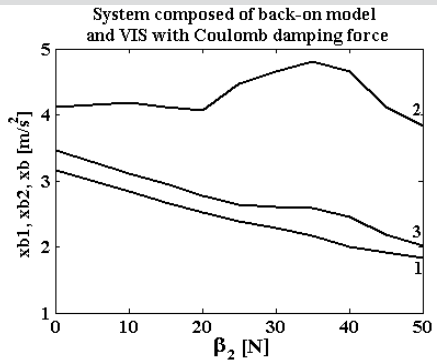

Fig. 26. Influence of parameter β_2 on accelerations: $1-\ddot{x}_1; 2-\ddot{x}_2; 3-\ddot{x}$

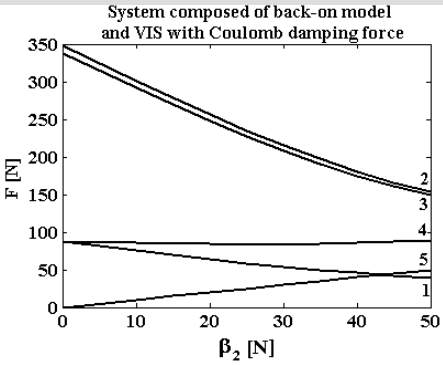

Fig. 27. Influence of parameter β_2 on forces: $1-F_{\alpha_m}; 2-F_{c_m}; 3-F_{\alpha_m}+F_{c_m}; 4-F_{\alpha_m}+F_{\beta_2}; 5-F_{\beta_2}$

Table 8. Numerical results of simulation for non-linear Coulomb force *T* ("back-on" model)

β_2	xb_1	xb_2	xb	x_1	x_2	x	x_2-x_1	x_1-x	x_2-x	$F_{\alpha m}$	F_{cm}	$F_{\alpha m}$+ F_{cm}	$F_{\alpha m}$ +$F_{\beta 2}$	$F_{\beta 2}$
0	3,17	4,12	3,46	0,03198	0,04076	0,03492	0,00879	0,00296	0,00584	87,2	347,6	336,8	87,2	0
10	2,85	4,19	3,11	0,02799	0,03564	0,03053	0,00766	0,00258	0,00512	75,6	300,6	291,4	85,6	10,0
15	2,66	4,12	2,95	0,02604	0,03316	0,02840	0,00713	0,00239	0,00478	69,9	278,1	269,4	84,9	15,0
20	2,53	4,07	2,78	0,02415	0,03076	0,02632	0,00661	0,00222	0,00445	64,3	256,2	248,1	84,2	19,9
25	2,39	4,47	2,63	0,02232	0,02844	0,02432	0,00614	0,00207	0,00413	58,8	235,2	227,2	83,7	24,9
30	2,28	4,67	2,61	0,02060	0,02625	0,02242	0,00574	0,00195	0,00385	53,9	215,4	207,7	83,8	29,9
35	2,17	4,81	2,60	0,01901	0,02428	0,02070	0,00537	0,00184	0,00359	49,9	197,4	190,2	84,8	34,8
40	2,00	4,66	2,46	0,01757	0,02246	0,01915	0,00499	0,00174	0,00332	46,2	180,6	174,9	86,0	39,8
45	1,92	4,12	2,18	0,01625	0,02077	0,01773	0,00461	0,00163	0,00304	42,6	165,8	160,8	87,3	44,7
50	1,84	3,84	2,01	0,01513	0,01937	0,01654	0,00428	0,00160	0,00285	39,3	154,2	149,0	89,0	49,7

4. DYNAMICS OF AHBM – VIS NON-LINEAR MODELS SUBJECTED TO RANDOM EXCITATION

In this part of the paper the results of the simulation analysis of the AHBM – VIS system subjected to narrow band (NBN) random acceleration excitation are presented. The "back--off" and "back-on" human body models seated on the linear and non-linear vibration isolation system were subjected to the narrow band noise acceleration excitation with r.m.s. values equal sequentially to four levels of acceleration amplitude $a_0 = 0.686$ [m/s^2], $2a_0$, $4a_0$, $8a_0$. The influence of the non-linearities given by the formulae (3), (4), (5), installed in the Kelvin – Voigt VIS was expressed, as the ratios of amplitude accelerations ($T_{xb}1$, T_{xb2}, T_{xb}), relative displacements (T_{x1-x}, T_{x2-x}, T_{x2-x1}), and total forces acting on seat mass, coming from model (T_{MOD}) and from VIS (T_{VIS}). The ratios were calculated for "back-off" and "back-on" models and listed correspondingly in Tables 9 and 10.

In Figures 28–31 the exemplary graphical illustrations of the ratios were shown for the "back-off" and "back-on" models and chosen non-linear force depicted by the formula (4). The figures show that the influence of the non-linear quadratic damping force increases with the value of the coefficient β_1 and the acceleration amplitude. In general, from Tables 9 and 10 one can conclude that, for the assumed numerical parameters of acceleration excitation and the AHBM – VIS model, the most visible changes are for specified accelerations and forces for the non-linearity depicted by the formula (4).

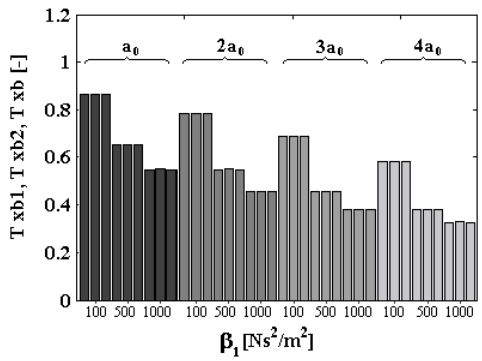

Fig. 28. System composed of "back-off" model and VIS with quadratic damping force

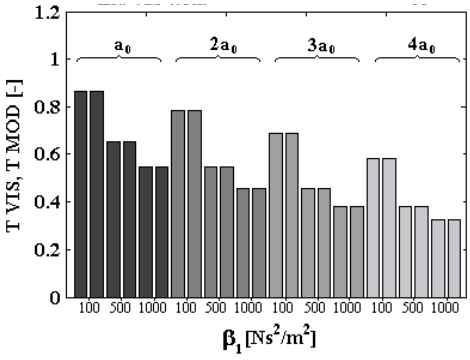

Fig. 29. System composed of "back-off" model and VIS with quadratic damping force

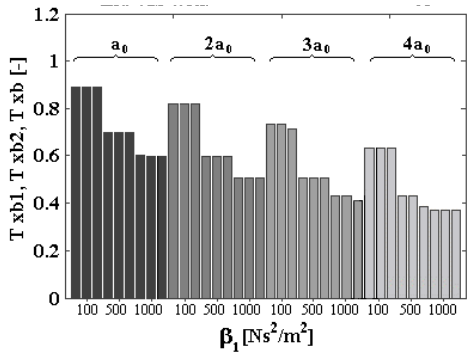

Fig. 30. System composed of "back-on" model and VIS with quadratic damping force

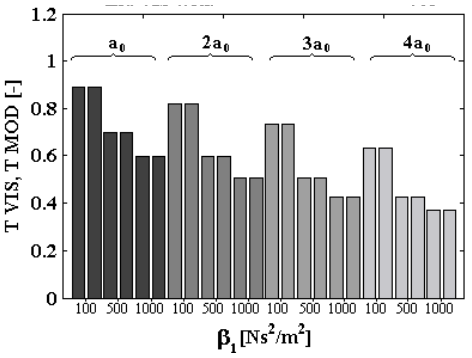

Fig. 31. System composed of "back-on" model and VIS with quadratic damping force

Table 9. Assumed numerical parameters of acceleration excitation

β_1	100			500			1000		
n a_0	Txb_1	Txb_2	Txb	Txb_1	Txb_2	Txb	Txb_1	Txb_2	Txb
a_0	0.8643	0.8643	0.8642	0.6523	0.6527	0.6523	0.5492	0.5499	0.5491
2 a_0	0.7839	0.7840	0.7839	0.5492	0.5500	0.5491	0.4564	0.4576	0.4562
4 a_0	0.6858	0.6861	0.6858	0.4564	0.4576	0.4562	0.3812	0.3831	0.3809
8 a_0	0.5818	0.5824	0.5817	0.3812	0.3831	0.3809	0.3259	0.3285	0.3254
β_2	10			20			40		
a_0	0.9644	0.9667	0.9672	0.9804	0.9816	0.9819	0.9897	0.9904	0.9905
2 a_0	0.9803	0.9816	0.9819	0.9897	0.9903	0.9905	0.9803	0.9816	0.9819
4 a_0	0.9897	0.9903	0.9905	0.9947	0.9950	0.9951	0.9973	0.9975	0.9975
8 a_0	0.9947	0.9950	0.9951	0.9973	0.9975	0.9975	0.9987	0.9987	0.9988
γ	100			500			1000		
a_0	0.8280	0.8449	0.8445	0.6410	0.6527	0.6523	0.9906	1.0082	1.0082
2 a_0	1.0163	1.0163	1.0026	1.0259	1.0260	1.0258	1.0082	1.0082	1.0082
4 a_0	1.0162	1.0163	1.0160	1.0259	1.0260	1.0258	1.0082	1.0082	0.9940
8 a_0	1.0162	1.0163	1.0160	1.0259	1.0260	1.0258	1.0082	1.0082	1.0082

β_1	100			500			1000		
n a_0	Tx_2-x_1	Tx_1-x	Tx_2-x	Tx_2-x_1	Tx_1-x	Tx_2-x	Tx_2-x_1	Tx_1-x	Tx_2-x
a_0	0.9988	0.9984	0.9993	0.9972	0.9964	0.9983	0.9966	0.9956	0.9980
2 a_0	0.9981	0.9976	0.9975	0.9966	0.9957	0.9980	0.9975	0.9950	0.9977
4 a_0	0.9974	0.9967	0.9985	0.9961	0.9951	0.9977	0.9958	0.9946	0.9975
8 a_0	0.9968	0.9959	0.9961	0.9958	0.9946	0.9955	0.9956	0.9944	0.9954
β_2	10			20			40		
a_0	0.9988	0.9878	0.9929	0.9994	0.9933	0.9961	0.9997	0.9965	0.9980
2 a_0	0.9994	0.9933	0.9961	0.9997	0.9965	0.9980	0.9994	0.9933	0.9961
4 a_0	0.9997	0.9965	0.9980	0.9998	0.9982	0.9990	0.9999	0.9991	0.9995
8 a_0	0.9999	0.9982	0.9990	0.9999	0.9991	0.9995	1.0000	0.9996	0.9998
γ	100			500			1000		
a_0	0.1389	0.1424	0.1355	1.0002	1.0003	1.0001	1.0001	1.0001	1.0001
2 a_0	1.0001	1.0001	1.0001	1.0002	1.0003	1.0001	1.0001	1.0001	1.0001
4 a_0	1.0001	1.0001	1.0001	1.0002	1.0003	1.0001	1.0001	1.0001	1.0001
8 a_0	1.0001	1.0001	1.0001	1.0002	1.0003	1.0001	1.0001	1.0001	0.9395

Table 9. cd

β_1	100		500		1000	
n a_0	T_{VIS}	T_{MOD}	T_{VIS}	T_{MOD}	T_{VIS}	T_{MOD}
a_0	0.8642	0.8642	0.6524	0.6524	0.5495	0.5494
2 a_0	0.7839	0.7839	0.5495	0.5494	0.4569	0.4567
4 a_0	0.6859	0.6858	0.4569	0.4567	0.3819	0.3816
8 a_0	0.5820	0.5819	0.3820	0.3816	0.3269	0.3264
β_2	10		20		40	
a_0	0.9642	0.9656	0.9802	0.9810	0.9896	0.9900
2 a_0	0.9801	0.9810	0.9895	0.9900	0.9801	0.9810
4 a_0	0.9831	0.9900	0.9947	0.9949	0.9973	0.9974
8 a_0	0.9946	0.9971	0.9973	0.9996	0.9986	1.0009
γ	100		500		1000	
a_0	1.0162	1.0161	1.0259	1.0259	1.0082	1.0082
2 a_0	1.0162	1.0161	1.0259	1.0259	1.0082	1.0082
4 a_0	1.0162	1.0161	1.0259	1.0259	1.0082	0.9988
8 a_0	1.0162	1.0161	1.0259	1.0082	0.9988	1.0127

Table 10. Assumed numerical parameters of the AHBM – VIS model

β_1	100			500			1000		
n a_0	Txb_1	Txb_2	Txb	Txb_1	Txb_2	Txb	Txb_1	Txb_2	Txb
a_0	0.8907	0.8907	0.8906	0.7000	0.6969	0.6997	0.6001	0.5998	0.5995
2 a_0	0.8210	0.8209	0.8209	0.6000	0.5998	0.5995	0.5067	0.5063	0.5058
4 a_0	0.7315	0.7314	0.7155	0.5067	0.5059	0.5058	0.4292	0.4287	0.4120
8 a_0	0.6320	0.6318	0.6316	0.4292	0.4287	0.3838	0.3714	0.3708	0.3694
β_2	10			20			40		
a_0	1.0225	1.0057	1.0187	1.0107	1.0024	1.0088	1.0051	1.0011	1.0042
2 a_0	1.0106	1.0024	1.0088	1.0051	1.0011	1.0042	1.0106	1.0024	1.0088
4 a_0	1.0051	1.0010	1.0042	1.0025	1.0005	1.0020	1.0012	1.0002	1.0010
8 a_0	1.0025	1.0005	1.0021	1.0012	1.0003	1.0010	1.0006	1.0001	1.0005
γ	100			500			1000		
a_0	0.5733	0.5707	0.5675	0.7591	0.7557	0.7588	1.0208	1.0207	1.0204
2 a_0	1.0160	1.0156	1.0152	1.0208	1.0207	1.0204	1.0064	1.0064	1.0063
4 a_0	1.0160	1.0156	1.0152	1.0208	1.0207	1.0204	1.0064	1.0064	1.0064
8 a_0	1.0160	1.0175	1.0152	1.0208	1.0225	1.0204	1.0064	1.0082	1.0063

β_1	100			500			1000		
n a_0	Tx_2-x_1	Tx_1-x	Tx_2-x	Tx_2-x_1	Tx_1-x	Tx_2-x	Tx_2-x_1	Tx_1-x	Tx_2-x
a_0	1.0000	1.0000	1.0000	1.0000	1.0000	0.9999	0.9999	1.0000	0.9999
2 a_0	1.0000	1.0000	0.9999	1.0000	1.0000	0.9999	1.0000	1.0000	0.9999
4 a_0	1.0000	1.0000	0.9999	1.0000	1.0000	0.9999	1.0000	1.0000	0.9999
8 a_0	1.0000	1.0000	0.9999	0.9999	1.0000	0.9998	0.9999	1.0000	0.9998
β_2	10			20			40		
a_0	0.9999	0.9997	1.0003	0.9999	0.9998	1.0001	0.9999	0.9999	1.0001
2 a_0	0.9999	0.9998	1.0000	0.9999	0.9999	1.0000	0.9999	0.9998	1.0000
4 a_0	1.0000	0.9999	1.0000	1.0000	1.0000	1.0000	1.0000	1.0000	1.0000
8 a_0	1.0000	0.9999	1.0000	1.0000	0.9999	1.0000	1.0000	0.9999	1.0000
γ	100			500			1000		
a_0	0.9999	1.0000	0.9999	1.0000	1.0000	1.0000	1.0000	1.0000	0.9995
2 a_0	1.0001	1.0000	1.0000	1.0001	1.0000	1.0000	1.0000	1.0000	1.0000
4 a_0	1.0000	1.0000	1.0000	1.0000	1.0000	1.0000	1.0000	1.0000	1.0000
8 a_0	1.0000	1.0000	1.0000	1.0000	1.0000	1.0000	1.0000	1.0000	1.0000

Table 10. cd

β_1	100		500		1000	
n a_0	T_{VIS}	T_{MOD}	T_{VIS}	T_{MOD}	T_{VIS}	T_{MOD}
a_0	0.8906	0.8906	0.6999	0.6998	0.5998	0.5997
2 a_0	0.8209	0.8209	0.5998	0.5997	0.5063	0.5061
4 a_0	0.7314	0.7314	0.5063	0.5055	0.4285	0.4283
8 a_0	0.6319	0.6310	0.4285	0.4277	0.3703	0.3695
β_2	10		20		40	
a_0	1.0229	1.0279	1.0127	1.0132	1.0053	1.0063
2 a_0	1.0110	1.0132	1.0054	1.0064	1.0110	1.0132
4 a_0	1.0053	1.0064	1.0026	1.0032	1.0013	1.0016
8 a_0	1.0068	1.0032	1.0013	1.0016	1.0007	1.0008
γ	100		500		1000	
a_0	1.0156	1.0155	1.0207	1.0206	1.0063	1.0063
2 a_0	1.0157	1.0155	1.0207	1.0206	1.0064	1.0064
4 a_0	1.0157	1.0156	1.0207	1.0206	1.0063	1.0064
8 a_0	1.0156	1.0155	1.0207	1.0206	1.0098	1.0063

5. CONCLUDING REMARKS

Functional active structures of human body models, due to changes of sitting positions, can lead to instability of the whole AHBM+VIS system. Seat modelling should be preceded by stability analysis. In case of the "back-on" model, as is shown in Figure 2, the biggest influence on the system stability have the values of the damping coefficient α_m and the mass m_0. Real seats are non-linear structures. The procedure of the simulation analysis is a very useful one in studies concerning the sensitivity of the vibration isolation system to the non-linear elements. It allows for fast estimation of influence of non-linearities and their parameters on isolation criteria without application, very often unfeasible, analytical approach. In the presented paper was shown, that in the considered cases most interesting are the results concerning the influence of the quadratic damping non-linearity and the coulomb non-linearity in case when the acceleration values of the mass m_0 change very sharply. In case when the power spectral density of random excitation acceleration has its maximum at the same frequency as in case of sinusoidal acceleration excitation the differences between the values of the measured amplitudes and forces depend on the form of non-linearity. The biggest differences were observed for quadratic damping.

References

[1] Amirouche F.M.L.: *Modeling of Human Reactions to Whole-Body Vibration.* Journal of Biomechanical Engineering, vol. 109, May 1987, 210–217

[2] Coermann R.R., Ziegenruecker G.H., Wittwer A.L., Von Gierke H.E.: *The Passive Dynamic Mechanical Properties of the Human Thorax-Abdomen System and the Whole Body System.* Aerospace Medicine, vol. 31, June 1960, 443–455

[3] Coermann R.R.: *Comparison of the Dynamic Characteristics of Dummies, Animals and Man.* Reprinted from Impact Acceleration Stress. Publication, No. 977, Nov. 1961, 173–184

[4] Coermann R.R.: *The Mechanical Impedance of the Human Body in Sitting and Standing Position at Low Frequencies.* Human Factors, 4(10) October, 1962, 227–253

[5] Cullmann A.: *Ein aktiver Schwingungsdummy des sitzenden Menschen.* Fortschr.-Ber. VDI-Reihe 12 Nr. 492, Düsseldorf, 2002

[6] Engel Z.: *Ochrona środowiska przed drganiami i hałasem.* Warszawa, Wydawnictwo Naukowe PWN 2001

[7] Garg D.P., Ross M.A.: *Vertical Mode Human Body Vibration Transmissibility.* IEEE Transactions on Systems, Man, and Cybernetics, No. 2, February 1976, 102–112

[8] Gierke H.E.: *Biodynamic Models and Their Applications.* The Journal of the Acoustical Society of America, 50, 1971, 1397–1413

[9] Gunston T., Griffin M.J.: *The Isolation Performance of a Suspension Seat Over a Range of Vibration Magnitudes Tested with an Anthropodynamic Dummy and Human Subjects.* Proceedings of Inter-Noise99, Florida, USA, Annex E

[10] Gunston T.P.: *Two methods of simulating a suspension seat cushion.* Proceedings of the 37th United Kingdom Group Meeting on Human Responses to Vibration, Loughborough University, September 18–20, 2002, England, 322–335

[11] Hopkins G.R.: *Nonlinear Lumped Parameter Mathematical Model of the Dynamic Response of the Human Body.* AMRL-TR-71-29, Wright-Patterson Air Force Base, Ohio, 649–669

[12] Kiene J., Meltzig-Thiel R., Schatte M.: *Results of the mathematical and mechanical modeling of the sitting man.* Strojnicki Casopis, 40, 1989, c. 2, 151–168

[13] Kowal J.: *Sterowanie drganiami.* Kraków, Wyd. Gutenberg 1996

[14] Książek M.: *Some Problems of Identification and Modelling of the Human Body, Man under Vibration, Suffering and Protection.* Proceedings of the International CISM-IFToMM-WHO Symposium, Udine, Italy, April 3–6, 1979, 200–209

[15] Książek M.: *Synteza aktywnych modeli ciała człowieka.* Materiały III Szkoły Układów Aktywnych, Zakopane, kwiecień 1997, 135–140

[16] Książek M.A.: *New active models of a sitting human body.* Proceedings of the 11th Conference of the European Society of Biomechanics, Toulouse, July 8–11, 1998, France, Journal of Biomechanics, vol. 31, Suppl. 1

[17] Książek M.A.: *Modelowanie i optymalizacja układu człowiek – wibroizolator – maszyna.* Seria Mechanika, nr 244, Kraków, Wyd. Politechnika Krakowska 1999

[18] Książek M. A.: *Active biomechanical models of a sitting human body.* Proceedings of the 34th United Kingdom Group Meeting on Human Responses to Vibration, Dunton, September 22–24, 1999, England

[19] Lewis C.H., Griffin M.J.: *Evaluating the vibration isolation of soft seat cushions using an active anthropodynamic dummy.* Journal of Sound and Vibration, vol. 253, 2002, 295–311

[20] Mansfield N.J., Griffin, M.J.: *Vehicle seat dynamics measured with an anthropodynamic dummy and human subjects.* Proceedings of Internoise 96 Congress, 30 July–2 August, Liverpool, 1996, UK, 1725–1730

[21] Muskian R., Nash, C.D.Jr.: *On Frequency-Dependent damping Coefficients in Lumped-Parameter Model of Human Beings.* Journal of Biomechanics, vol. 9, 1976, 339–342
[22] Paddan G.S., Griffin M.J.: *Transmission of vibration through the human body to the head: a summary of experimental data.* ISVR Technical Report, No. 218, 1993
[23] Payne P.R., Band E.G.U.: *A Four-Degree-of Freedom Lumped Parameter Model of the Seated Human Body.* AMRL-TR-70-35, Wright-Patterson Air Force Base, Ohio, 1971, 1–111
[24] Potiemkin B.A., Frolov K.V.: *Non-linear Effects Connected With The Spatial Vibrations of Biomechanical Systems.* Man Under Vibration. Suffering and Protection, Proceedings of the International CISM-IFToMM-WHO Symposium, Udine, Italy, April 3–6, 1979, 228–234
[25] Rosen J., Arcan M.: *Modeling the Human Body/Seat System in a Vibration Environment.* Journal of Biomechanical Engineering, April 2003, vol. 125, 223–231
[26] Suggs C.W., Abrams C.F.Jr.: *Simulation of Whole Body Dynamics.* Proc. 5th Ann. Southwestern Symp. on Systems Theory, March, 1973, 176–180
[27] Smith S.D.: *Resonance behaviour of the human exposed to whole - body vibration.* United Kingdom Informal Group on Human Response to Vibration, Southampton, 28–30 September, 1992, 41–52
[28] Yamakawa S.: *Vibration Data analysis of Automobiles.* Statistics for Engineering and Physical Science, The Practice of Time Series Analysis, Chapter 14, Editors: H. Akaike, G. Kitagawa, Springer-Verlag New York Inc., 1999
[29] Yoshimura T., Tamaoki G.: *A study of dynamics and modeling of human body exposed to multi-dimensional excitation.* Proceedings of Internoise 96 Congress, 30 July–2 August 1996, Liverpool, UK, 1743–1748
[30] Wei L., Griffin M.J.: *Mathematical models for the apparent mass of the seated human body exposed to vertical vibration.* Journal of Sound and Vibration, 212(1), 1998, 855–874
[31] Wei L., Griffin M.J.: *Mathematical model for the mechanical impedance of the human body exposed to vertical vibration.* Journal of Sound and Vibration, 212(5), 1998, 855–874
[32] Wei L., Griffin M.J.: *Effect of subject weight on predictions of seat cushion transmissibility.* Proceedings of the 35th United Kingdom Group Meeting on Human Responses to Vibration, Southampton, September 13–15, 2000, England, 17–28
[33] Wiesner A., Donnadieu A., Berthoz A.: *A Biomechanical Model of Man for the Study of Vehicle Seat and Suspension.* The International Journal of Production Research, vol. 3, No. 4, 1964, 285–315